Carbohydrate Polymers 90 (2012) 1299–1304

Contents lists available at SciVerse ScienceDirect

Carbohydrate Polymers

journal homepage: www.elsevier.com/locate/carbpol

Sequence analysis of the sulfated rhamno-oligosaccharides derived from a sulfated rhamnan

Hongyan Li[a,b], Wenjun Mao[a,*], Yin Chen[a], Sumei Ren[a], Xiaohui Qi[a], Yanli Chen[a], Chunqi Zhao[a], Na Li[a], Chunyan Wang[a], Cong Lin[a], Mengxia Yan[a], Jimiao Shan[a]

[a] Key Laboratory of Marine Drugs, Ministry of Education, Institute of Marine Drug and Food, Ocean University of China, Qingdao 266003, People's Republic of China
[b] College of Chemistry and Environment Science, Hebei University, Baoding 071002, People's Republic of China

ARTICLE INFO

Article history:
Received 10 February 2012
Received in revised form 8 June 2012
Accepted 27 June 2012
Available online 5 July 2012

Keywords:
Sulfated rhamno-oligosaccharide
Sequence
NMR
ES-CID MS/MS

ABSTRACT

Three sulfated rhamno-oligosaccharides, designated O1, O2 and O3, were obtained by mild acid hydrolysis of the sulfated rhamnan and purified by gel-permeation chromatography. On the basis of one- and two-dimensional nuclear magnetic resonance (1D, 2D NMR) spectroscopic analyses, the oligosaccharide O1 was characterized to be α-L-Rha*p*-(2SO4)-(1 → 3)-α-L-Rha*p*. The fragmentation pattern of the homogeneous disaccharide in the product ion spectra was recognized by negative-ion electrospray tandem mass spectrometry with collision-induced dissociation (ES-CID MS/MS). With the principles established, the sequences of the oligosaccharides O2 and O3 were deduced to be α-L-Rha*p*-(2SO4)-(1 → 3)-α-L-Rha*p*-(1 → 3)-α-L-Rha*p*, and α-L-Rha*p*-(2SO4)-(1 → 3)-α-L-Rha*p*-(1 → 3)-α-L-Rha*p*-(1 → 3)-α-L-Rha*p* ($2SO_4$), respectively. The investigation demonstrated that the sulfated rhamnan-derived oligosaccharides were novel sulfated oligosaccharides different from those of other polysaccharides-degraded from algae, and it could be possible to determine the sequence of the sulfated rhamno-oligosaccharides directly from the glycosidic cleavage fragmentation in the product ion spectra.

1. Introduction

Sulfated polysaccharides from Monostromaceae species exhibited potent anticoagulant activity and became considerable biomedical interest (Hayakawa et al., 2000; Maeda, Uehara, Harada, Sekiguchi, & Hiraoka, 1991; Mao et al., 2008). The structure of the sulfated polysaccharide will indubitably play an indispensable role in the understanding of its anticoagulant activity. For a long period of time, methylation analysis has been the major method for the structural investigation of the sulfated polysaccharide (Harada & Maeda, 1998; Lee, Yamagaki, Maeda, & Nakanishi, 1998; Mao et al., 2009; Zhang et al., 2008). The methylation of sulfated polysaccharide does not always yield reliable proportions of methylated alditols because the steric hindrance of the sulfate esters does not allow complete methylation of these polymers (Mulloy, Ribeiro, Alves, Vieira, & Mourao, 1994; Patankar, Oehninger, Barnett, Williams, & Clark, 1993). Recently, an in-depth nuclear magnetic resonance (NMR) spectroscopic analysis on the sulfated polysaccharide was completed (Lee, Koizumi, Hayashi, & Hayashi, 2010; Li et al., 2011). The sulfated polysaccharide from *M. latissimum* consisted of (1 → 3)-linked α-L-rhamnopyranose, (1 → 2)-linked α-L-rhamnopyranose and (1 → 2,3)-linked α-L-rhamnopyranose residues in a molar ratio of 4:1:1, and the sulfate groups were substituted at C-2 of the (1 → 3)-linked α-L-rhamnopyranose and C-3 of the (1 → 2) -linked α-L-rhamnopyranose residues (Li et al., 2011). The soluble polysaccharides isolated from Monostromaceae species constitute a family of sulfated rhamnans with differences in their linkage and sulfation patterns. The complete assignment of NMR spectra of the sulfated polysaccharide is very difficult. The structural heterogeneity of the sulfated polysaccharides with respect to linkage pattern and sulfate position is a major limitation to elucidate its precise structure. Sequence determination of the sulfated polysaccharide remains a huge challenge.

Mass spectrometry has become increasingly important for analysis of polysaccharides due to its high sensitivity, high accuracy and fast processing (Penn, Cancilla, & Lebrilla, 1996; Reinhold, Reinhold, & Costello, 1995; Viseux, Hoffmann, & Domon, 1997). The sequence analysis of derivatized and underivatized oligosaccharides has been completed by mass spectrometry (Bahr, Pfenninger, Karas, & Stahl, 1997; Cancilla, Gaucher, Desaire, & Leary, 2000; Chai, Piskarev, & Lawson, 2001; Huang & Riggin, 2000). Negative-ion electrospray tandem mass spectrometry with collision-induced dissociation (ES-CID MS/MS) has been successfully used for sequence determination of various types of carbohydrate molecules (Briggs, Keck, Ma, Lau, & Jones, 2009; Chai, Lawson, & Piskarev, 2002; Zhang, Yu,

* Corresponding author. Tel.: +86 532 8203 1560; fax: +86 532 8203 3054.
E-mail address: wenjunmqd@hotmail.com (W. Mao).

0144-8617/$ – see front matter © 2012 Elsevier Ltd. All rights reserved.
http://dx.doi.org/10.1016/j.carbpol.2012.06.076

Zhao, Liu, & Guan, 2006). Unique fragmentation can arise at certain monosaccharide residues with specific linkages under CID MS/MS conditions, and these provide important information on sequence and linkages (Daniel et al., 2007; Zaia, Mcclellan, & Costello, 2001). So far, sequence analysis of the sulfated rhamno-oligosaccharides by ES-CID MS/MS has not been found.

In the present paper, three sulfated rhamno-oligosaccharide fragments were prepared by mild acid hydrolysis of the sulfated polysaccharide (Li et al., 2011). The sequence of oligosaccharide O1 was first elucidated by detailed NMR spectroscopic analyses, and then the fragmentation pattern of the oligosaccharide O1 in the product ion spectra was recognized on the basis of negative-ion ES-CID MS/MS spectroscopy. The principles established were applicable to sequence determination of the sulfated rhamno-oligosaccharides O2 and O3.

2. Material and methods

2.1. Materials

Sulfated rhamnan was extracted from *Monostroma latissimum* (an artificial breeding in China). Sephadex G10 was from Pharmacia Bioscience (Uppsala, Sweden). Bio-Gel P-4 was from BioRad (Richmond, CA). Silica Gel 60 high performance thin layer chromatography (HPTLC) plates (with aluminum backing) were from Merck (Darmstadt, Germany).

2.2. Preparation of the sulfated rhamno-oligosaccharides by mild acid hydrolysis

Sulfated rhamnan was isolated from *M. latissimum* according to the method described by Li et al. (2011). The sulfated rhamnan (250 mL, 1 mg/mL) was hydrolyzed with 0.1 mol/L H_2SO_4 at 60 °C for 3 h. The hydrolysate was neutralized with 1.0 mol/L NaOH, concentrated under reduced pressure at 40 °C, and same volume of 95% ethanol was added. The supernatant was recovered by centrifugation at 4500 rpm for 30 min, concentrated, desalted on a Sephadex G10 column (1.6 cm × 100 cm), and further fractionated with a Bio-Gel P-4 column (1.6 cm × 100 cm) by elution with 0.2 mol/L NH_4HCO_3 and detection by refractive index. The oligosaccharide fractions were collected, and further purified on the Bio-Gel P-4 column. Three oligosaccharide fractions were obtained, designated as O1, O2 and O3.

2.3. High performance thin layer chromatography

The purity of oligosaccharide was checked on a silica gel HPTLC plate (2 cm × 2 cm) developed with a solvent system of *n*-propanol/water/triethylamine (60:30:0.7, v/v/v). The developed plates were stained by dipping in diphenylamine/aniline/phosphoric acid reagent for 2 s, and heated at electric furnace for color development.

2.4. Nuclear magnetic resonance spectroscopy

The sample was deuterium exchanged by successive freeze-drying steps in 99% D_2O, and then dissolved in 0.5 mL of 99.98% D_2O. ^1H NMR and ^{13}C NMR spectra were recorded at 23 °C using a JEOL JNM-ECP 600 MHz spectrometer equipped with 5 mm multinuclear probe with inverse detection. Chemical shifts are expressed in ppm using acetone as internal standard at 2.225 ppm for ^1H and 31.45 ppm for ^{13}C. ^1H–^1H correlated spectroscopy (COSY), ^1H–^{13}C heteronuclear multiple quantum coherence spectroscopy (HMQC) and ^1H–^{13}C heteronuclear multiple bond correlation spectroscopy (HMBC) and ^1H–^1H nuclear overhauser effect spectroscopy (NOESY) experiments were also carried out.

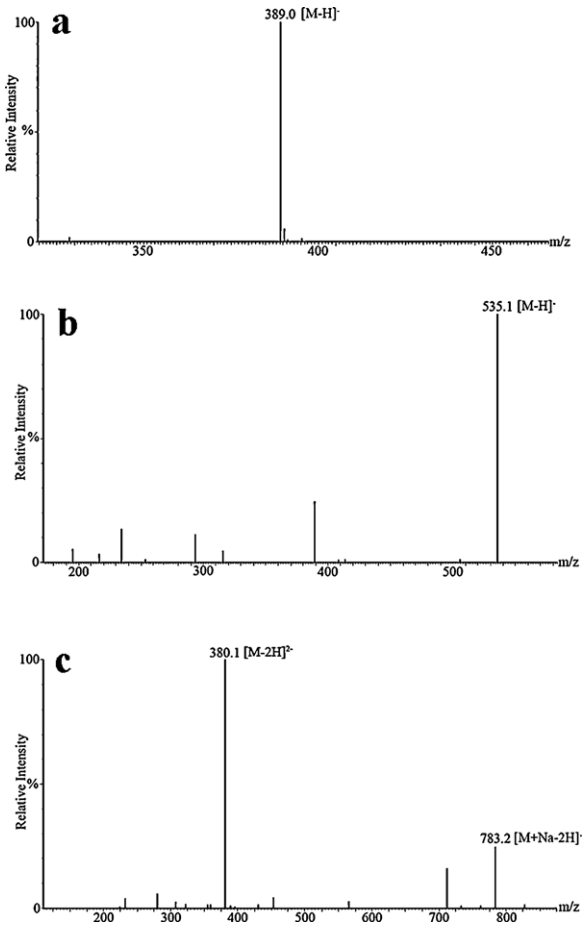

Fig. 1. Negative-ion ESMS spectra of the sulfated rhamno-oligosaccharides derived from the sulfated rhamnan. (a) O1 spectrum; (b) O2 spectrum; (c) O3 spectrum.

2.5. Electrospray mass spectrometry

Negative-ion electrospray mass spectrometry (ESMS) analysis was performed on a Micromass Q-Tof Ultima instrument (Waters, Manchester, UK). Nitrogen was used as the desolvation and nebulizer gas at a flow rate of 250 L/h and 15 L/h, respectively. The source temperature was 80 °C and the desolvation temperature was 150 °C. Samples were dissolved in acetonitrile/H_2O (1:1, v/v), typically at a concentration of 10–20 pmol/μL, of which 10 μL was loop-injected. The mobile phase (acetonitrile/H_2O, 1:1, v/v) was delivered by a syringe pump at a flow rate of 10 μL/min. The capillary voltage maintained at 3 kV, and the cone voltage was 30–100 V, depending on the size of the oligosaccharides. For CID MS/MS product-ion scanning, argon was used as the collision gas at a pressure of 1.7 bar and the collision energy was adjusted between 20 and 50 eV for optimal sequence information.

3. Results and discussion

3.1. Preparation of the sulfated rhamno-oligosaccharides

The sulfated rhamno-oligosaccharides were produced by mild acid hydrolysis of the sulfated rhamnan, and further purified by gel-filtration chromatography. The high performance thin layer chromatography analysis showed that each oligosaccharide migrated as a single band (Supplemental Fig. 1). From the

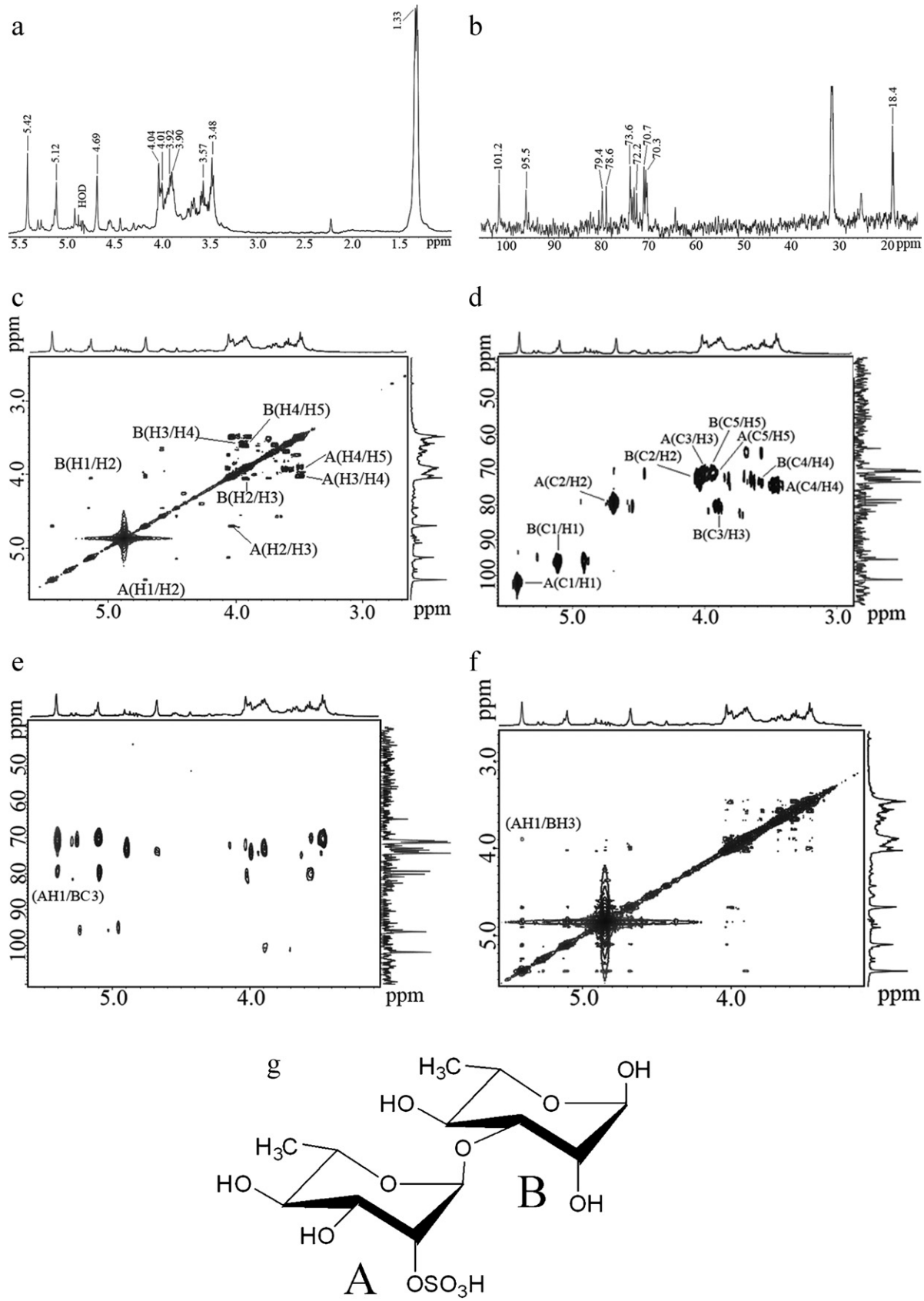

Fig. 2. NMR spectra of the rhamno-disaccharide O1 derived from the sulfated rhamnan. Spectra were performed at 23 °C on a JEOL ECP 600 MHz spectrometer. Chemical shifts are expressed in ppm using acetone as internal standard at 2.225 ppm for ^{1}H and 31.45 ppm for ^{13}C. (a) ^{1}H NMR spectrum; (b) ^{13}C NMR spectrum; (c) ^{1}H–^{1}H COSY spectrum; (d) ^{1}H–^{13}C HMQC spectrum; (e) ^{1}H–^{13}C HMBC spectrum; (f) ^{1}H–^{1}H NOESY spectrum; (g) proposed sequence of the rhamno-disaccharide O1 derived from the sulfated rhamnan. The rhamnose residues on the nonreducing and reducing terminal were named as A and B, respectively.

Table 1
^{1}H and ^{13}C chemical shifts for the oligosaccharide O1.

Rhamnosyl	^{1}H and ^{13}C chemical shifts[a]					
	H1/C1	H2/C2	H3/C3	H4/C4	H5/C5	H6/C6
A						
α-L-Rha-(1→	5.42	4.69	4.01	3.48	3.92	1.33
	101.2	78.6	70.7	73.6	70.3	18.4
B						
→3)-α-L-Rha	5.12	4.04	3.90	3.57	3.92	1.33
	95.5	72.2	79.4	72.7	70.3	18.4

[a] The spectra were performed at 23 °C on a JEOL ECP 600 MHz spectrometer. Chemical shifts are expressed in ppm using acetone as internal standard at 2.225 ppm for ^{1}H and 31.45 ppm for ^{13}C.

negative-ion ESMS spectrum of O1 (Fig. 1a), the oligosaccharide O1 was identified to be a monosulfated rhamno-disaccharide. In addition, the oligosaccharide O2 was deduced to be a monosulfated rhamno-trisaccharide (Fig. 1b), and the oligosaccharide O3 was proposed to be a disulfated rhamno-tetrasaccharide (Fig. 1c).

3.2. Sequence determination of the oligosaccharide O1 by NMR spectroscopy analysis

In the ^{1}H NMR spectrum of the disaccharide O1 (Fig. 2a), two major anomeric proton signals at 5.42 and 5.12 ppm were assigned to α-rhamnopyranosyl units. The proton signal at 1.33 ppm was attributed to the proton of CH_3 group of the rhamnose residues. In the anomeric region of ^{13}C NMR spectrum (Fig. 2b), two carbon resonances occurring at 101.2 and 95.5 ppm were attributed to C-1 of non-reducing and reducing α-rhamnopyranosyl units, respectively. The α-anomeric configuration of rhamnopyranose residues was also deduced from H-5 signal at 3.92 ppm and C-5 signal at 70.3 ppm (Cassolato et al., 2008). The high-field signal at 18.4 ppm was attributed to the C-6 of rhamnosyl units.

As a matter of assignment convenience, the rhamnose residues at nonreducing and reducing terminal in the disaccharide O1 were defined as **A** and **B**, respectively. The ^{1}H–^{1}H COSY spectrum of the disaccharide O1 gave various proton correlations of **A** and **B** residues (Fig. 2c). The ^{1}H–^{13}C HMQC spectrum afforded some of the correlations between carbon and proton signals with the sugar residues, and elaborated the site of sulfate ester in sugar residues and the linkage patterns between sugar residues. In the ^{1}H–^{13}C HMQC spectrum of the disaccharide O1 (Fig. 2d), the anomeric proton signal at 5.42 ppm with its correlated anomeric carbon signal at 101.2 ppm were attributed to the **A** residue. The anomeric proton signal at 5.12 ppm was related to the C-1 signal at 95.5 ppm, which was assigned to the **B** residue. In addition, the H-2 signal at 4.69 ppm of **A** showed the correlation with the C-2 signal at 78.6 ppm of **A**, suggesting the sulfate ester was in the C-2 position of **A**. The H-3 signal at 3.90 ppm of **B** was correlated with the C-3 signal at 79.4 ppm of **B**, and indicated the presence of (1 → 3)-linked rhamnopyranose residues.

The ^{1}H–^{13}C HMBC (Fig. 2e) and ^{1}H–^{1}H NOESY spectra (Fig. 2f) further confirmed some of the correlations between carbon and proton signals within the sugar residues, and the sequence of the sugar residues. The anomeric proton signal at 5.42 ppm of **A** was correlated with the C-3 signal at 79.4 ppm of **B** in the ^{1}H–^{13}C HMBC spectrum. The anomeric proton signal at 5.42 ppm of **A** was related to the H-3 signal at 3.90 ppm of **B** in the ^{1}H–^{1}H NOESY spectrum. Thus, the (1 → 3)-linked pattern between **A** and **B** was proved. The assignments of the proton and carbon chemical shifts of the sulfated disaccharide were listed in Table 1. The proposed sequence of the disaccharide O1 was shown in Fig. 2g.

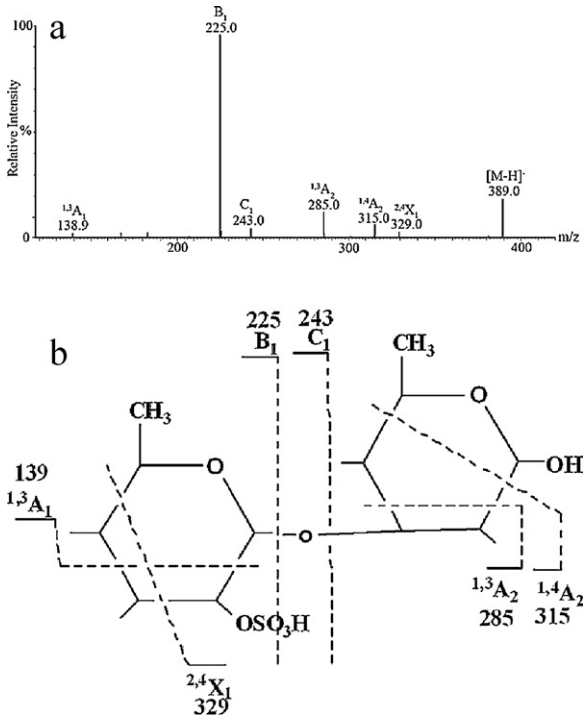

Fig. 3. Negative-ion ES-CID MS/MS product ion spectrum and assignments of the ions of the rhamno-disaccharide O1. (a) Negative-ion ES-CID MS/MS product ion spectrum; (b) assignments of the ions of the rhamno-disaccharide O1. The sequence is shown to indicate the proposed fragmentations.

3.3. Fragmentation pattern of the oligosaccharide O1 by negative-ion ES-CID MS/MS

Due to the anionic nature of sulfate, the detailed sequences of the sulfated rhamno-oligosaccharides O1, O2 and O3 were detected by negative-ion ES-CID MS/MS. The nomenclature used to define the fragmentations of oligosaccharide is based on that introduced by Domon and Costello (1988). For the negative-ion ES-CID MS/MS, $[M-H]^-$ was used as precursors for optimal sequence information. The disaccharide O1 was used first for investigation of fragment patterns, and the principles established were then used for sequence determination of oligosaccharides O2 and O3.

The product-ion spectrum of *m/z* 389.0 in the negative-ion mode gave the detailed information of the disaccharide structure (Fig. 3a). The major ion *m/z* 225 was produced from single glycosidic bond cleavage and could be assigned as B_1. The weak ions of *m/z* 243 (C_1) arised from cleavage at carbon–carbon bond of the saccharide ring. The ions at *m/z* 139 and 329 were assigned to $^{1,3}A_1$ and $^{2,4}X_1$, respectively, indicating the sulfate ester was at the C-2. The fragment $^{1,3}A_2$ ion of *m/z* 285 and $^{1,4}A_2$ ion of *m/z* 315 of the cleavage in the saccharide ring further proved the linkage of (1 → 3)-α-L-Rha*p*. The position of the sulfate ester and the linkage pattern obtained from the fragmentation of the ES-CID MS/MS were in agreement with those of NMR results. The fragmentation pattern of the disaccharide O1 was established (Fig. 3b).

3.4. Sequence determination of the oligosaccharide O2 by negative-ion ES-CID MS/MS

In the ES-CID MS/MS spectrum of O2 (Fig. 4a), the major ion *m/z* 535.1 showed similar feature to that of the disaccharide. The trisaccharide gave product ion spectra with fragments B1 (*m/z* 225), C1 (*m/z* 243), B2 (*m/z* 371), and C2 (*m/z* 389) ions of the glycosidic bond cleavage, and also generated $^{1,3}A_2$ (*m/z* 285), $^{1,4}A_2$ (*m/z* 315), $^{1,3}A_3$ (*m/z* 431), $^{1,4}A_3$ (*m/z* 461) and $^{2,4}X_2$ (*m/z* 475) ions

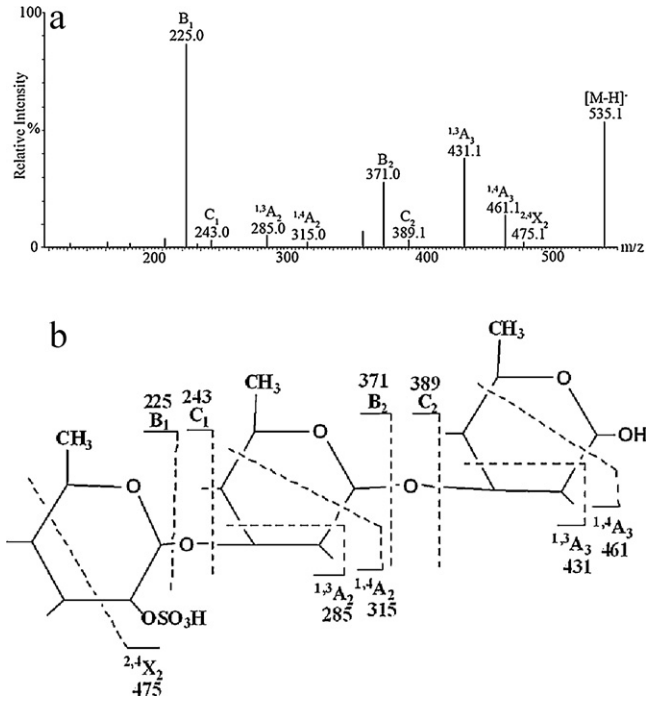

Fig. 4. Negative-ion ES-CID MS/MS product ion spectrum and sequence of the rhamno-trisaccharide O2. (a) Negative-ion ES-CID MS/MS product ion spectrum; (b) sequence of the rhamno-trisaccharide O2. The assignments of the ions of the rhamno-trisaccharide O2 is shown in the sequence.

from cross-ring cleavage. According to the established principles from the sulfated disaccharide O1, the sulfate ester of the trisaccharide was at the C-2 of the rhamnose on the non-reducing end, the linkage pattern was 3-linked rhamnose. The sequence of the monosulfated trisaccharide was deduced to be α-L-Rha*p*-(2SO4)-(1 → 3)-α-L-Rha*p*-(1 → 3)-α-L-Rha*p* (Fig. 4b).

3.5. Sequence determination of the oligosaccharide O3 by negative-ion ES-CID MS/MS

As sulfate ester groups are labile, the loss of sulfate ester during collision-induced association was prevented by sodium adduction. Here, the singly charged molecular ion $[M+Na-2H]^-$ at *m*/*z* 783.2 was used as the precursor ion for the ES-CID MS/MS analysis. The ES-CID MS/MS of the disulfated tetrarhamnose O3 was shown in Fig. 5a. As expected, its linear sequence could be readily derived from the major fragment ions B_1 *m*/*z* 225, C_1 *m*/*z* 243, B_2 *m*/*z* 371, C_2 *m*/*z* 389, B_3 *m*/*z* 517 and C_3 *m*/*z* 535 arising by glycosidic cleavages. The cross ring cleavage ions $^{1,3}A_2$ (*m*/*z* 285), $^{1,4}A_2$ (*m*/*z* 315), $^{1,3}A_3$ (*m*/*z* 431), $^{1,4}A_3$ (*m*/*z* 461), $^{1,3}A_4$ (*m*/*z* 577), $^{1,4}A_4$ (*m*/*z* 709), $^{1,3}A_4$ (*m*/*z* 679) and $^{2,4}X_3$ (*m*/*z* 621) were also detected. The fragment ion $^{2,4}X_3$ (*m*/*z* 621) was produced on the basis of the loss of SO_3Na. The sulfation positions were deduced to be at the C-2 of both the reducing and the non-reducing end of the rhamnose, and the linkage was 3-linked tetrasaccharide. Thus, the sequence of the tetrasaccharide O3 was presumed to be α-L-Rha*p*-(2SO4)-(1 → 3)-α-L-Rha*p*-(1 → 3)-α-L-Rha*p*-(1 → 3)-α-L-Rha*p* ($2SO_4$) (Fig. 5b).

The sulfated rhamno-oligosaccharides O1, O2, and O3 appeared to be oligosaccharides with structural characteristics different from those of other oligosaccharides from algae (Yu et al., 2006; Zhang et al., 2006). It was noted that the partial acid hydrolysis of the sulfated polysaccharide gave rise to oligosaccharides with

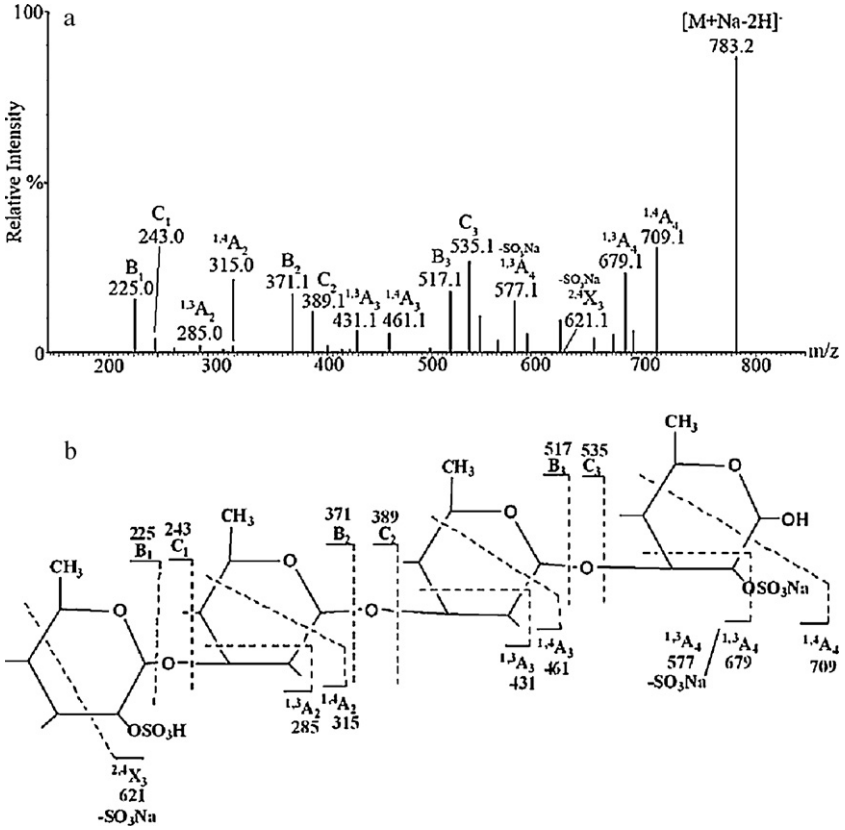

Fig. 5. Negative-ion ES-CID MS/MS product ion spectrum and sequence of rhamno-tetrasaccharide O3. (a) Negative-ion ES-CID MS/MS product ion spectrum; (b) sequence of rhamno-tetrasaccharide O3 derived from the sulfated rhamnan. The assignments of the ions of the rhamno-tetrasaccharide O3 is shown in the sequence.

(1 → 3)-linked glycosidic linkage, possibly was due to the main backbone of the sulfated polysaccharide from *M. latissimum* consisted of (1 → 3)-α-L-Rha*p*, and the molar ratio of (1 → 3)-linked α-L-rhamnopyranose and (1 → 2)-linked α-L-rhamnopyranose was about 4:1 (Li et al., 2011). In addition, the hydrolysis of (1 → 3)-linked glycosidic linkages may be easier than that of (1 → 2)-linked glycosidic linkages. For extending the results toward a rational interpretation of the negative-ion ESMS fragmentation of oligosaccharides derived from the sulfated rhamnan, the sulfated rhamno-oligosaccharides O2 and O3 are being prepared for further NMR spectroscopic analyses. In addition, preparation of the sulfated rhamno-oligosaccharides with different glycosidic linkages will be required for in-depth negative-ion ES-CID MS/MS spectroscopic study.

4. Conclusion

The sulfated rhamno-oligosaccharides O1, O2 and O3 were successfully prepared by controlled acid hydrolysis of the sulfated rhamnan and purified by gel-permeation chromatography. Based on detailed NMR spectroscopic analyses, the sequence of O1 was deduced to consist of α-L-Rha*p*-(2SO4)-(1 → 3)-α-L-Rha*p*, and the fragmentation pattern of O1 in the product ion spectra was identified on the basis of negative-ion ES-CID MS/MS spectrometry. With the aid of the principles established, the sequences of O2 and O3 were characterized to be α-L-Rha*p*-(2SO4)-(1 → 3)-α-L-Rha*p*-(1 → 3)-α-L-Rha*p* and α-L-Rha*p*-(2SO4)-(1 → 3)-α-L-Rha*p*-(1 → 3)-α-L-Rha*p*-(1 → 3)-α-L-Rha*p* ($2SO_4$), respectively. The sulfated rhamnan-derived oligosaccharides were novel sulfated oligosaccharides different from those of other polysaccharides-degraded from algae. Due to the anionic nature of sulfate, negative-ion detection of sulfated rhamno-oligosaccharides is the usual choice for high-sensitively detection. The negative-ion ES-CID MS/MS gives an efficient method for the sequence analysis of the sulfated rhamno-oligosaccharides which reveals the pattern of substitution including the sulfated groups and glycosidic linkage pattern. A further investigation on negative-ion ES-CID MS/MS of the sulfated rhamno-oligosaccharides is still in progress.

Acknowledgements

This work was supported by the National Natural Science Foundation of China (41076086) and the Doctoral Program of Higher Education of China (20090132110015), the Science and Technology Development Program of Shandong Province, China (2010GHY10509) and National Oceanographic Center of Qingdao, China. The authors gratefully thank Dr Chai in Glycosciences Laboratory, Faculty of Medicine, Imperial College London, United Kingdom for his help in this work.

Appendix A. Supplementary data

Supplementary data associated with this article can be found, in the online version, at http://dx.doi.org/10.1016/j.carbpol.2012.06.076.

References

Bahr, U., Pfenninger, A., Karas, M., & Stahl, B. (1997). High-sensitivity analysis of neutral underivatized oligosacchardies by nanoelectrospray mass spectrometry. *Analytical Chemistry*, *69*, 4530–4535.

Briggs, J. B., Keck, R. G., Ma, S., Lau, W., & Jones, A. J. S. (2009). An analytical system for the characterization of highly heterogeneous mixtures of *N*-linked oligosaccharides. *Analytical Biochemistry*, *389*, 40–51.

Cancilla, M. T., Gaucher, S. P., Desaire, H., & Leary, J. A. (2000). Combined partial acid hydrolysis and electrospray ionization–mass spectrometry for the structural determination of oligosaccharides. *Analytical Chemistry*, *72*, 2901–2907.

Cassolato, J. E. F., Noseda, M. D., Pujol, C. A., Pellizzari, F. M., Damonte, E. B., & Duarte, M. E. R. (2008). Chemical structure and antiviral activity of the sulfated heterorhamnan isolated from the green seaweed *Gayralia oxysperma*. *Carbohydrate Research*, *343*, 3085–3095.

Chai, W. G., Piskarev, V., & Lawson, A. M. (2001). Negative-ion electrospray mass spectrometry of neutral underivatized oligosaccharides. *Analytical Chemistry*, *73*, 651–657.

Chai, W. G., Lawson, A. M., & Piskarev, V. (2002). Branching pattern and sequence analysis of underivatized oligosaccharides by combined MS/MS of singly and doubly charged molecular ions in negative-ion electrospray mass spectrometry. *Journal of the American Society for Mass Spectrometry*, *13*, 670–679.

Daniel, R., Chevolot, L., Carrascal, M., Tissot, B., Mourao, P. A. S., & Abian, J. (2007). Electrospray ionization mass spectrometry of oligosaccharides derived from fucoidan of *Ascophyllum nodosum*. *Carbohydrate Research*, *342*, 826–834.

Domon, B., & Costello, C. E. (1988). A systematic nomenclature for carbohydrate fragmentation in FAB-MS/MS spectra of glycoconjugates. *Glycoconjugate Journal*, *5*, 397–409.

Harada, N., & Maeda, M. (1998). Chemical structure of antithrombin-active rhamnan sulfate from *Monostroma nitidum*. *Bioscience, Biotechnology, and Biochemistry*, *62*, 1647–1652.

Hayakawa, Y., Hayashi, T., Lee, J. B., Srisomporn, P., Maeda, M., Ozawa, T., et al. (2000). Inhibition of thrombin by sulfated polysaccharides isolated from green algae. *Biochimica et Biophysica Acta (BBA)-Protein Structure and Molecular Enzymology*, *1543*, 86–94.

Huang, L. H., & Riggin, R. M. (2000). Analysis of nonderivatized neutral and sialylated oligosaccharides by electrospray mass spectrometry. *Analytical Chemistry*, *72*, 3539–3546.

Lee, J. B., Koizumi, S., Hayashi, K., & Hayashi, T. (2010). Structure of rhamnan sulfate from the green alga *Monostroma nitidum* and its anti-herpetic effect. *Carbohydrate Polymers*, *81*, 572–577.

Lee, J. B., Yamagaki, T., Maeda, M., & Nakanishi, H. (1998). Rhamnan sulfate from cell walls of *Monostroma latissimum*. *Phytochemistry*, *48*, 921–925.

Li, H. Y., Mao, W. J., Zhang, X. L., Qi, X. H., Chen, Y., Chen, Y. L., et al. (2011). Structural characterization of an anticoagulant-active sulfated polysaccharide isolated from green alga *Monostroma latissimum*. *Carbohydrate Polymers*, *85*, 394–400.

Maeda, M., Uehara, T., Harada, N., Sekiguchi, M., & Hiraoka, A. (1991). Heparinoid-active sulfated polysacchardies from *Monostroma nitidum* and their distribution in the chlorophyta. *Phytochemistry*, *30*, 3611–3614.

Mao, W. J., Fang, F., Li, H. Y., Zhang, H. J., Qi, X. H., Sun, H. H., et al. (2008). Heparinoid-active two sulfated polysaccharides isolated from marine green algae *Monostroma nitidum*. *Carbohydrate Polymers*, *74*, 834–839.

Mao, W. J., Li, H. Y., Zhang, H. J., Qi, X. H., Sun, H. H., Chen, Y., et al. (2009). Chemical characteristic and anticoagulant activity of the sulfated polysaccharide isolated from *Monostroma latissimum* (Chlorophyta). *International Journal of Biological Macromolecules*, *44*, 70–74.

Mulloy, B., Ribeiro, A. C., Alves, A. P., Vieira, R. P., & Mourao, P. A. S. (1994). Sulfated fucans from echinoderms have a regular tetrasaccharide repeating unit defined by specific patterns of sulfation at the O-2 and O-4 positions. *Journal of Biological Chemistry*, *269*, 22113–22123.

Patankar, M. S., Oehninger, S., Barnett, T., Williams, R. L., & Clark, G. F. (1993). A revised structure for fucoidan may explain some of its biological activities. *Journal of Biological Chemistry*, *268*, 21770–21776.

Penn, S. G., Cancilla, M. T., & Lebrilla, C. B. (1996). Collison-induced dissociation of branched oligosacchardie ions with analysis and calculation of related dissociation thresholds. *Analytical Chemistry*, *68*, 2331–2339.

Reinhold, V. N., Reinhold, B. B., & Costello, C. E. (1995). Carbohydrate molecular weight profiling, sequence, linkage, and branching data: ES-MS and CID. *Analytical Chemistry*, *67*, 1772–1784.

Viseux, N., Hoffmann, E. D., & Domon, B. (1997). Structural analysis of permethylated oligosaccharides by electrospray tandem mass spectrometry. *Analytical Chemistry*, *69*, 3193–3198.

Yu, G. L., Zhao, X., Yang, B., Ren, S. M., Guan, H. S., Zhang, Y. B., et al. (2006). Sequence analysis of sulfated carrageenan-derived oligosaccharides by high-sensitivity negative-ion electrospray tandem mass spectrometry. *Analytical Chemistry*, *78*, 8499–8505.

Zaia, J., Mcclellan, J. E., & Costello, C. E. (2001). Tandem mass spectrometric determination of the 4S/6S sulfation sequence in chondroitin sulfate oligosaccharides. *Analytical Chemistry*, *73*, 6030–6039.

Zhang, H. J., Mao, W. J., Fang, F., Li, H. Y., Sun, H. H., Chen, Y., et al. (2008). Chemical characteristics and anticoagulant activities of a sulfated polysaccharide and its fragments from *Monostroma latissimum*. *Carbohydrate Polymers*, *71*, 428–434.

Zhang, Z. Q., Yu, G. L., Zhao, X., Liu, H. Y., & Guan, H. S. (2006). Sequence analysis of alginate-derived oligosaccharide by negative-ion electrospray tandem mass spectrometry. *Journal of the American Society for Mass Spectrometry*, *17*, 621–630.